

Magnetic topology during the reconnection process in a kinked coronal loop

H. Baty

Observatoire Astronomique, 11 Rue de l'Université, 67000 Strasbourg, France (baty@astro.u-strasbg.fr)

Received 9 March 2000 / Accepted 6 June 2000

Abstract. The magnetic topology change that arises during the evolution of the kink instability in a solar coronal loop is studied using a three-dimensional MHD simulation in cylindrical geometry. The initial structure is an axisymmetric twisted magnetic flux tube carrying a vanishing axial electric current, that has primarily evolved towards a kinked configuration containing an intense current concentration along the loop. Consequently, the ensuing evolution becomes resistive allowing a stationary reconnection process to occur (Baty 2000). The system finally reaches a relaxed configuration of lower magnetic energy with three topologically distinct regions. Indeed, the original highly twisted central region is transformed into two interwoven flux tubes with field lines having a small amount of twist within each tube. This first region is surrounded by a weakly non axisymmetric annular flux tube that is embedded into the original potential magnetic field. Using mappings of field lines along the loop from one photospheric end, we draw a schematic description of the magnetic topology change in terms of the initial distributions of the twist and/or of the axial current density.

Key words: instabilities – magnetic fields – Magnetohydrodynamics (MHD) – molecular data – Sun: corona

1. Introduction

It is well established that the development of the kink instability in coronal loops may play a crucial role in the dynamics of the solar corona. Indeed, a kinked magnetic flux tube experiences a disruption that could explain compact loop flares (Velli et al. 1997, Arber et al. 1999, Amari & Luciani 1999). It also releases, at the same time, a significant amount of magnetic energy that could contribute to heat the solar corona (Galsgaard & Nordlund 1997, Baty 2000 hereafter referred to as Paper I).

Of particular interest here, are solar loops having magnetic field lines that are locally twisted in the central region and carrying no net axial current (Lionello et al. 1998, Baty et al. 1998, Arber et al. 1999). This class of configurations would result from a vortex photospheric flow acting on an initially potential magnetic field and leading to a sequence of quasi-equilibria with a gradual build-up of the twist (Mikic et al. 1990). When

the amount of twist injected in the loop exceeds a critical value, the configuration becomes kink unstable (Raadu 1972, Hood & Priest 1979, Einaudi et al. 1983). The early evolution of this instability then generates a high electric current concentration along the loop length (Baty 1997, Velli et al. 1997, Arber et al. 1999). When sufficiently large magnetic field gradients are created, the ensuing evolution becomes resistive with the occurrence of a magnetic reconnection process (Einaudi et al. 1997, Lionello et al. 1998, Arber et al. 1999, Paper I). In Paper I, we have obtained a steady-state reconnection of field lines consistent with results predicted by the well known two-dimensional Sweet-Parker model, in spite of the three-dimensional (3D) character of the process. We have also found that the system finally reaches a relaxed state of lower magnetic energy, releasing more than 50 percent of the free energy stored in the initial configuration.

In the present paper, we propose to examine in details the magnetic topology change that arises during the reconnection. Some aspects of this problem have been previously addressed in cylindrical geometry approximation (Bazdenkov & Sato 1998) and also in the true 3D geometry (Amari & Luciani 1999, 2000). An important result obtained in these studies is the splitting of the initial flux tube into two topologically distinct pieces. Indeed, Amari & Luciani (1999) have shown that the final state is a relaxed configuration consisting of two almost untwisted flux tubes confined by an overlaying arcade. Contrary to these papers where a photospheric flow is applied to the footpoints to continuously inject twist in the loop, we introduce an initial twisted configuration that is already kink unstable. Therefore, we focus on the topological change resulting from the non linear evolution of the kink instability alone, the whole evolution of the loop configuration with the photospheric flow effect being beyond the scope of the present paper. This is an important point in order to contribute to the understanding of the 3D reconnection phenomenon in the solar corona, that has begun to be studied only recently (Priest 1997 and references therein).

As in most of the previously mentioned references, we have carried out numerical simulations in the cylindrical geometry approximation. We have followed the non linear resistive evolution of a single magnetic equilibrium representative of an initially unstable coronal loop, using optimal values for the dissipation coefficients in our MHD evolution code, SCYL.

The paper is organized as follows. The physical and numerical loop models are presented in Sect. 2. The next section is devoted to the numerical results. Finally, a schematic description of the magnetic topology change is given and conclusions are drawn.

2. The loop model

The cylindrical flux tube as well as the numerical procedure used in this study are described in details in Paper I. However, we briefly recall here the main features of the coronal loop model.

An initially axisymmetric equilibrium with a force-free magnetic field and a vanishing plasma pressure is assumed. The twist, that has been numerically calculated, is a decreasing function of the radial coordinate with a maximum value of 6.1π on the axis (see Fig. 2 in Paper I). As one can see in Fig. 1, an internal twisted flux tube of length L situated inside $r/a = 0.4$ is embedded into a potential region having a vanishing azimuthal magnetic field component. A perfectly conducting wall is also placed at the outer radial boundary $r/a = 1$ for the numerical procedure requirements. This loop configuration is kink unstable because the amount of twist exceeds a critical value (of 5.6π on the axis, see Paper I). The first stage of the development of the kink mode has been then followed (see the results reported in paper I) using our code SCYL with a vanishing resistivity coefficient in the MHD equations. This ideal phase is characterized by a strong deformation of the internal region of the loop while the more external (potential) region is unaltered (see Fig. 2). An intense helical-like current concentration is also forming along the loop. When the smaller magnetic length scale reaches the grid resolution, the ensuing evolution becomes resistive and the use of a non zero resistivity coefficient (in MHD equations) dominating the residual numerical resistivity is necessary to pursue the simulation (Arber et al. 1999, Paper I).

Therefore, as the starting point of the present work, a constant and uniform resistivity coefficient $\eta \simeq 10^{-4}$ (in our dimensionless units) is introduced at a given time $T = 23.7t_a$ (t_a being the radial Alfvén crossing time defined in Paper I) corresponding to a kinked state that gives a (maximum) current density amplitude of two times the initial equilibrium one. This resistivity value is an optimal one as higher values would lead to the unrealistic diffusion of the whole equilibrium while smaller values lead to a considerable amount of time of cpu computation (Paper I). A viscosity coefficient equal to the resistivity one is also used. We have then completed the time evolution of the system until a relaxed state of lower magnetic energy was obtained. As explained in Paper I and by Arber et al. (1999), this final state is characterized by the dissipation of the current concentration that is representative of the available free magnetic energy.

3. The numerical results

In order to investigate the change of the magnetic topology that arises during the reconnection process, we have examined the connectivity of different field lines. As the coronal perturbations

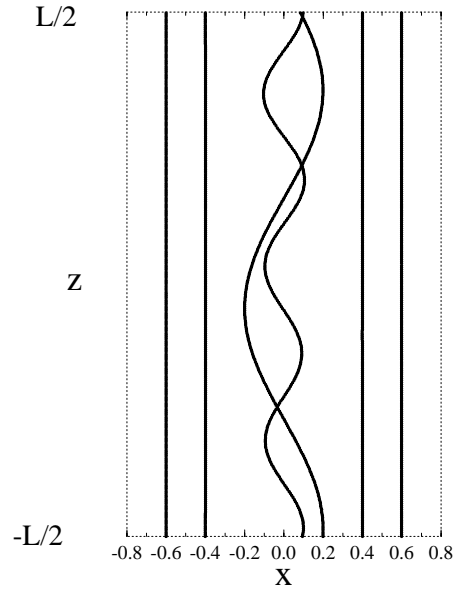


Fig. 1. Projection on the (x, z) plane of several magnetic field lines anchored at different positions $x = r/a \cos(\theta)$ at the photosphere (at $z = \pm L/2$), for the initial twisted (axisymmetric) configuration. The cylindrical coordinate system (r, θ, z) is used.

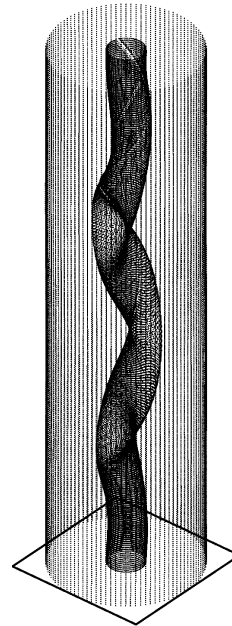


Fig. 2. A 3D view of the ideal kinked configuration (starting point of the present simulation) showing many field lines anchored at two radial positions $r/a = 0.1$ and 0.4 at the photosphere.

are assumed to vanish at the photosphere (inertial anchoring), each line can be identified by its radial and azimuthal coordinates at one photospheric end-plate. The two photospheric planes are situated at $z = \pm L/2$. As the axial component of the magnetic field remains positive everywhere in the coronal medium (for the present configuration) during the evolution of the system, each field line can be obtained by numerically inte-

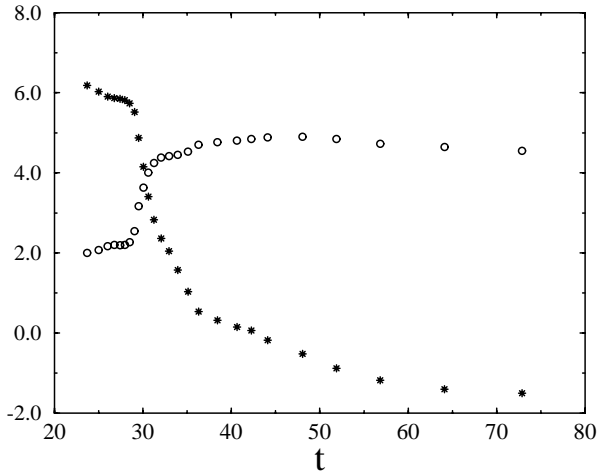


Fig. 3. The final mapping $\mathbf{r}_+(L/2)$ as a function of time, giving the radial (circles) and azimuthal (stars) coordinates at $z = L/2$ of a given field line originating from $\mathbf{r}_0(-L/2) = (0.1a, 0)$. The results are reported in arbitrary units in order to be plotted on the same graph.

grating the following field line equation from one photospheric end towards the other:

$$\frac{d\mathbf{r}}{dz} = \frac{\mathbf{B}_p}{B_z}, \quad (1)$$

where $\mathbf{r}(z) = (r(z), \theta(z))$ defines the intersection of the line with a $z = \text{constant}$ coronal plane. \mathbf{B}_p and B_z are the perpendicular and axial magnetic field components respectively. Using an initial condition $\mathbf{r}_0(-L/2)$ at the photospheric plane situated at $z = -L/2$, the solution to Eq. (1) gives a point $\mathbf{r}_+(z)$ at a given altitude z and a final point $\mathbf{r}_+(L/2)$ at the other photospheric end. Consequently, $\mathbf{r}_+(z)$ and $\mathbf{r}_+(L/2)$ define (direct) partial and final mappings respectively. Inverse partial and final mappings given by $\mathbf{r}_-(z)$ and $\mathbf{r}_-(-L/2)$ can be also obtained by integrating backward Eq. (1) and using an initial condition $\mathbf{r}_0(L/2)$ at the other photospheric plane situated at $z = L/2$.

First, we have followed the final mapping $\mathbf{r}_+(L/2)$ of a single field line, anchored at $\mathbf{r}_0(-L/2) = (0.1a, 0)$, as a function of time. The results are plotted in Fig. 3. One can easily see the drastic change of the coordinates at $t = 29t_a$ indicating the occurrence of the reconnection process through this change of field line connectivity. The beginning of the reconnecting event is determined by the time at which the field line trajectory intersects the current layer.

Second, we have investigated the direct partial mapping $\mathbf{r}_+(0)$ (i.e. to the loop apex) of three sets of field lines arranged in three photospheric circles given by $\mathbf{r}_0(-L/2) = (0.1a, \theta)$, $(0.15a, \theta)$, and $(0.2a, \theta)$, for the ideal kinked configuration. 1000 equidistant θ values situated in the range $[0, 2\pi]$ have been selected. The results plotted in Fig. 4, show that the two internal circles are transformed into two ovoid curves with an off-axis displacement of the magnetic axis. This is not the case for the more external lines which remain on an almost unaltered circle. This distorted topology is in agreement with surfaces shown in Fig. 2. Note that the inverse partial mapping $\mathbf{r}_-(0)$ obtained with the same initial conditions at $z = L/2$ would lead to points

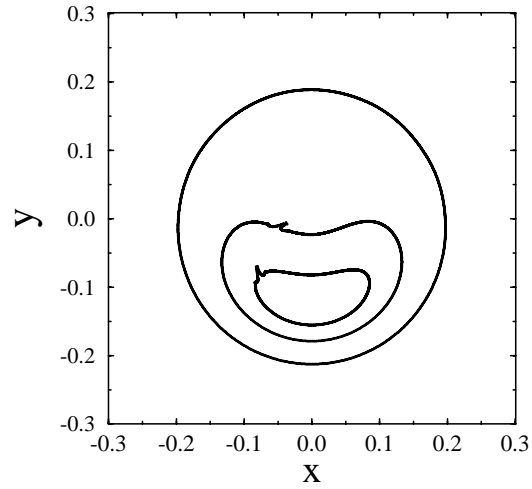


Fig. 4. The direct partial mapping to the loop apex $\mathbf{r}_+(0)$ (in cartesian coordinates) of three sets of magnetic field lines originating from $\mathbf{r}_0(-L/2) = (0.1a, \theta)$, $(0.15a, \theta)$, and $(0.2a, \theta)$ for the ideal kinked configuration.

lying on the same curves as in Fig. 4, and the final mapping $\mathbf{r}_+(L/2)$ would give circular curves corresponding to these initial conditions. This is due to the impossibility for the topology to change in ideal MHD.

Focusing now on the set of field lines originating from $\mathbf{r}_0(-L/2) = (0.1a, \theta)$ (again 1000 equidistant θ values between 0 and 2π are considered), we have examined (direct and inverse) partial mappings $\mathbf{r}_\pm(0)$ during the evolution of the configuration. The results are plotted in Fig. 5 at four times including the saturation. One can easily see that the points obtained from the direct and inverse mappings lie now on two different curves which do not coincide. This means that the initial topology is destroyed and the field lines are re-arranging due to the reconnection. Moreover, the two curves encompass two regions that are separating as time goes on. This result is confirmed by the 3D view of Fig. 6, which shows that two well separated interwoven surfaces are finally obtained for the relaxed state. We have checked that similar results are obtained for other sets of field lines starting from more internal circular curves (with radii $r_0 < 0.1a$) at the photospheric end-plates, and that the resulting mappings give then two interwoven tubes of different nested surfaces. We have found that the two flux tubes wrap one around each other as well as around the original axis with an angle of order 1.5π . This angle represents the helicity of each tube's axis, and it is also known as the writhe (Berger & Field 1984). This writhe value results from the deformation induced by the kink (see Fig. 2). As concerns the twist of the field lines within each tube, small values situated in the range $[0, \pi/2]$ have been obtained. Therefore, the field lines have lost most of their initial amount of twist during the reconnection process, in agreement with previous results (Einaudi et al. 1997, Amari & Luciani 1999).

The preceding result on the transformation into two separated flux tubes cannot be true for all the field lines of the nu-

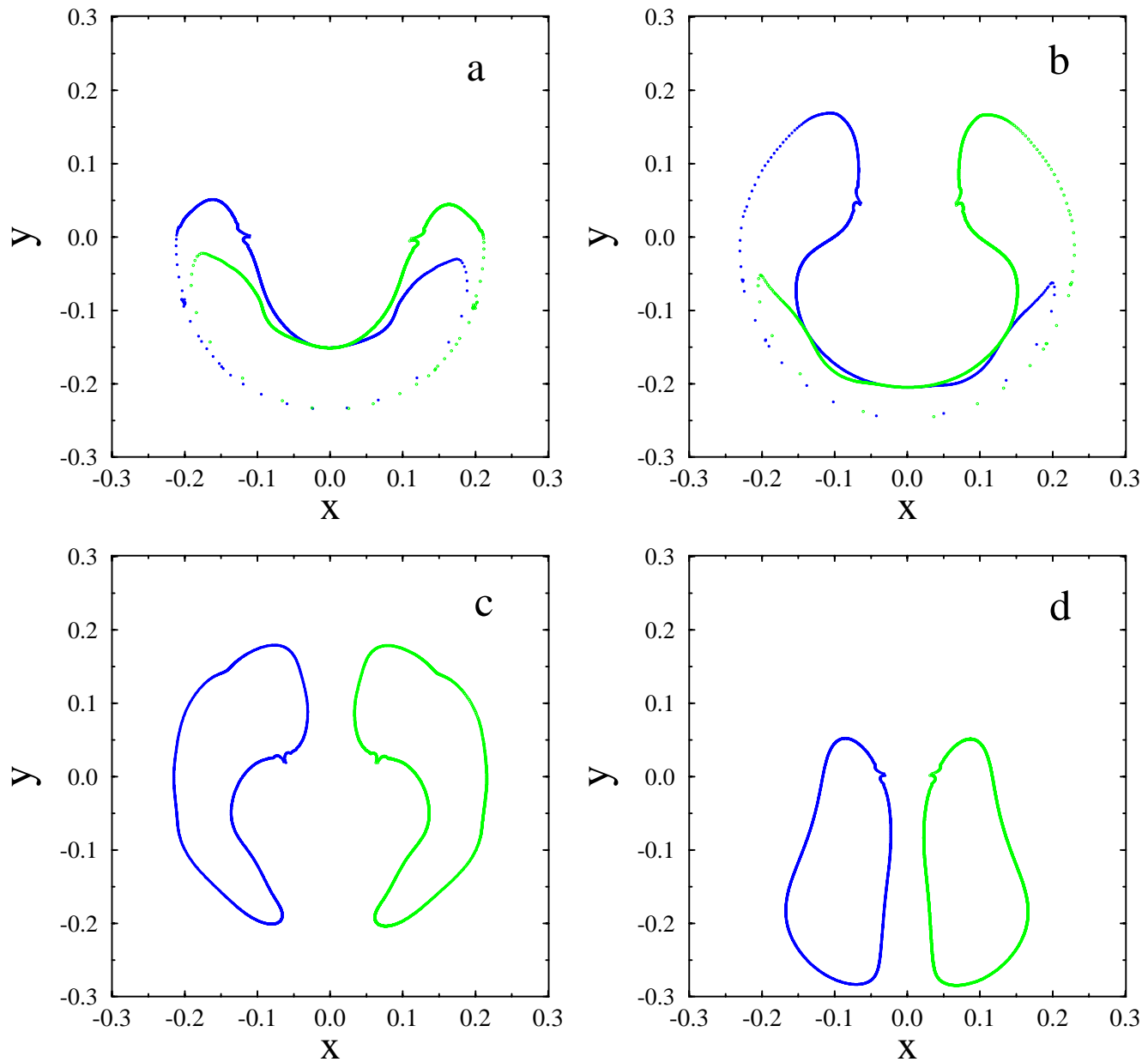


Fig. 5a–d. The partial mappings to the loop apex $r_{\pm}(0)$ of a set of field lines originating from a circular arrangement $r_0 = (0.1a, \theta)$ at the two photospheric ends $z = -L/2$ (green circles) and $z = L/2$ (blue stars), for an early resistive phase $t = 27.4t_a$ **a**, during the reconnection at $t = 29.5t_a$ **b** and $t = 31t_a$ **c**, and for the final relaxed state $t = 65t_a$ **d**.

merical flux tube, as at least the external potential region should remain unchanged (Einaudi et al. 1997). Therefore, we have investigated the partial mappings $r_{\pm}(0)$ using the initial conditions $r_0 = (0.2a, \theta)$ at $z = \pm L/2$, again with 1000 equidistant θ values lying on a closed circular curve. The results that are plotted in Fig. 7 for the final relaxed configuration, show that the two curves do not encompass (now) two well separated regions. However, some of the field lines are clearly connected to the region occupied by the two interwoven flux tubes. Selecting only a given range of θ values smaller than 2π , it is then possible to obtain two non closed curves that form a single closed one as one can see in the schematic mappings of Fig. 8c (region II). The

corresponding field lines form a single weakly non axisymmetric surface that surrounds the double flux tubes structure. This means that this second region is an annular flux tube. We have also found that the field lines situated in this second region have no twist.

The separation of these two topologically distinct regions can be made by using the initial conditions $r_0(\pm L/2)$ for the direct and inverse mappings. Indeed, we have found that the internal region containing the two well separated flux tubes corresponds to field lines obtained with footpoints arranged in circles with small radii at one photospheric end. More precisely, it is determined with mappings using initial conditions $r_0/a < 0.14$

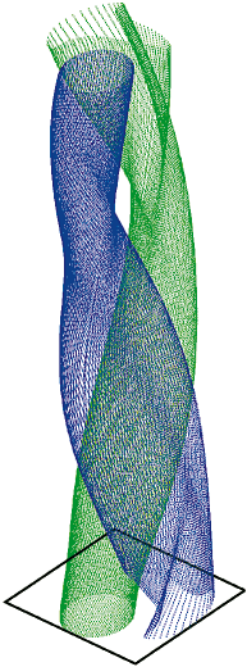


Fig. 6. A 3D view of field lines corresponding to mappings of Fig. 5d.

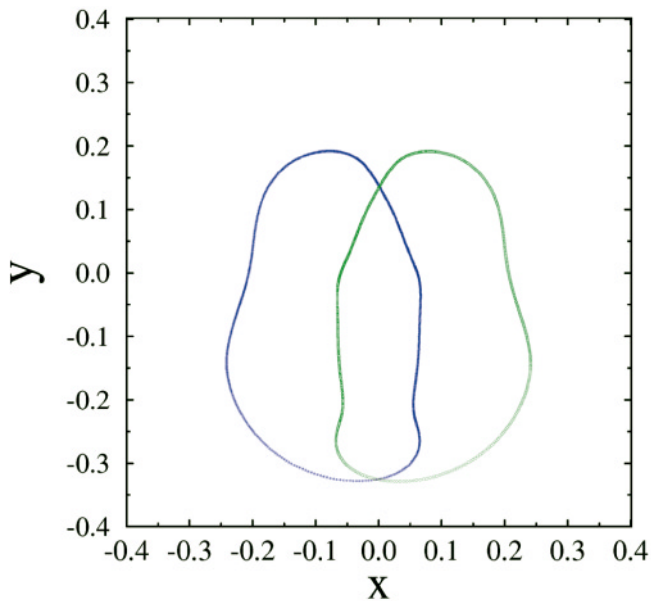


Fig. 7. Same as in Fig. 5d for $r_0 = (0.2a, \theta)$

and all the θ values in the range $[0, 2\pi]$ at $z = \pm L/2$. A separatrix surface can then be obtained from the critical radius $r_c/a = 0.14$. We have found that this value is correlated to the current distribution of the initial axisymmetric equilibrium. Indeed, it corresponds to the radius at which the axial current density reverses sign. We have also found that this value is correlated to the radius defining the region within which the initial field lines are highly twisted. We believe that this result remains true for a general axisymmetric configuration carrying a zero axial electric current, meaning that it is possible to predict the gross features of the magnetic topology of the relaxed state in

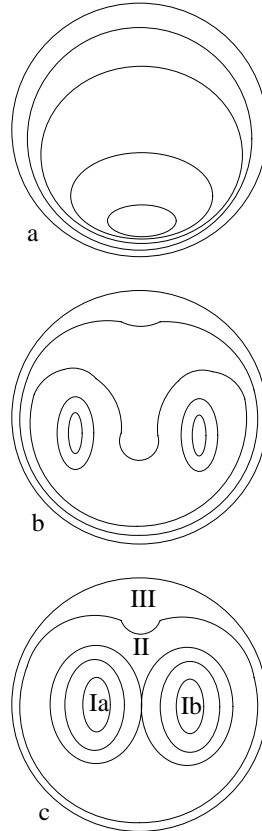


Fig. 8a–c. Schematic partial mappings to the loop apex of 5 set of field lines originating from circular arrangements at the two photospheric ends $z = \pm L/2$ for the ideal kinked state **a**, during the resistive phase **b**, and for the final relaxed state **c**. Closed and non closed circles are used for lines situated in regions I and II respectively.

terms of the equilibrium parameters defining the initially unstable twisted loop. We have finally checked that the field lines situated in the external potential region are not affected by the process, defining then a third region.

4. Conclusion

In this paper, we have considered the resistive evolution of a cylindrical coronal loop configuration that is kink unstable. We have assumed an initial axisymmetric flux tube carrying no net axial current with twisted magnetic field lines in the central region. We have then studied the change of the magnetic topology during the second stage of the evolution that is a reconnection process.

While previous results have shown the stationary character of the phenomenon in agreement with the Sweet-Parker model (Paper I), we have obtained that the internal field lines experiment reconnecting events when their trajectory intersects the current concentration region that has been formed during the early ideal phase.

We have examined the connectivity of field lines through the use of direct and inverse mappings, obtained by integrating a field line equation along the loop length from one photo-

spheric end towards the other. The results can be summarized by drawing a schematic description of partial (direct and inverse) mappings to the loop apex for three states: the ideal kinked configuration (a), during the reconnection (b), and the final relaxed state (c). We have shown that the configuration evolves towards a relaxed state containing three topologically distinct regions. First, an internal region where the initially highly twisted field lines originating from closed circular arrangements with small enough radii $r < r_c$ at each photospheric end, is progressively fully transformed into two interwoven flux tubes having a small amount of twist. We can then define a region I as one can see in Fig. 8c. The two flux tubes are labelled Ia and Ib in correspondence with initial conditions at $z = -L/2$ and $z = L/2$, respectively. A second more peripheral region (II) is also obtained with field lines originating from non closed circular arrangements (with $r > r_c$) at each photospheric plane. Indeed, only a given range of azimuthal positions smaller than 2π at the photosphere must be taken into account to form the curves in this region. This second region is a weakly non axisymmetric annular flux tube, giving partial mappings to the loop apex which consist of closed curves with two branches (in correspondence with the two sets of initial conditions at $z = -L/2$ and $z = L/2$). The field lines obtained from the remaining azimuthal positions at the photosphere are in fact connected to region I or to inner lines of region II. Finally, these two regions remain embedded in the external potential region that is unaltered by the process. We also found that the critical radius r_c coincides with the site at which the axial component of the current density of the initial axisymmetric configuration reverses. It also corresponds to the radius defining the region within which the twist was maximum. We believe that this result is a general feature of loop configurations carrying no net axial current.

However, in cases of finite current loops, the final relaxed state should be probably less well ordered as suggested by the numerical results obtained by Einaudi et al. (1997).

A similar two flux tubes configuration has been recently obtained by Amari & Luciani (1999) using a 3D simulation of a curved twisted loop embedded in an external potential magnetic field. However, these authors have not investigated in details the magnetic topology change, making then the comparison with our results difficult. We can, nevertheless, conclude that the cylindrical geometry approximation used here probably gives the essential features of the phenomenon. We then hope that our results can serve as a useful guideline to understand the 3D reconnection phenomenon in the solar corona.

Acknowledgements. The numerical calculations were performed on the CRAY C98 at I.D.R.I.S., Orsay (France). The author thanks Jean Heyvaerts for fruitful discussions, and the anonymous referee for fruitful comments.

References

- Amari T., Luciani J.F., 1999, ApJ 515, L81
- Amari T., Luciani J.F., 2000, Phys. Rev. Lett. 84, 1196
- Arber T.D., Longbottom A.W., Van der Linden R.A.M., 1999, ApJ 517, 990
- Bazdenkov S., Sato T., 1998, ApJ 500, 966
- Baty H., 1997, A&A 318, 621
- Baty H., Einaudi G., Lionello G., Velli M., 1998, A&A 333, 313
- Baty H., 2000, A&A 353, 1074
- Berger M.A., Field G.B., 1984, published in Journal of Fluid Mechanics 147, 133
- Einaudi G., Van Hoven G., 1983, Solar Phys. 99, 163
- Einaudi G., Lionello R., Velli M., 1997, Adv. Space Res. 19, 1875
- Galsgaard K., Nordlund A., 1997, J.G.R. 102, 219
- Hood A.W., Priest E.R., 1979, Solar Phys. 64, 303
- Lionello R., Velli M., Einaudi G., Mikic Z., 1998, ApJ 494, 840
- Mikic Z., Schnack D.D., 1990, ApJ 437, 851
- Priest E.R., 1997, Phys. Plasmas 4, 1945
- Raadu M.A., 1972, Solar Phys. 22, 425
- Velli M., Lionello R., Einaudi G., 1997, Solar Phys. 172, 257